J. Inst. Eng. India Ser. E (January–June 2015) 96(1):45–53
DOI 10.1007/s40034-015-0059-z

ORIGINAL CONTRIBUTION

Studies on Fragrance Delivery from Inorganic Nanocontainers: Encapsulation, Release and Modeling Studies

Shailesh Adinath Ghodke · Shirish Hari Sonawane · Bharat Apparao Bhanvase · Satyendra Mishra · Kalpana Shrikant Joshi

Received: 17 October 2014 / Accepted: 2 February 2015 / Published online: 27 March 2015

Abstract The present work deals with encapsulation of fragrance molecule in inorganic nanocontainers substrate and investigation of its prolonged release at different pH condition. The nanocontainers used were aluminosilicate clay (Halloysite) having cylindrical shape with outside diameter in the range of 30–50 nm, 15 nm lumen and length equal to 800 ± 300 nm. Rosewater absolute was used as a sample fragrance for loading in nanocontainer and delivery purpose. The fragrance loaded nanocontainers were coated with a thin layer of polyelectrolyte i.e. Polyacrylic Acid (PAA). The structural characteristics of prepared nanocontainers were determined by using Fourier Transform Intrared Spectroscopy (FTIR), Thermal Gravimetric Analysis (TGA) and UV spectroscopy analysis. Release of fragrance molecules in the aqueous medium was monitored for 24 h. The fragrance release was found to be responsive as the amount of fragrance release increases with increase in pH value from 3 to 7. Fragrance release has been studied by using various permeation kinetic models such as zero order, first order, Hixson–Crowell, Higuchi, Korsmeyer–Peppas and Hopfenberg models. Korsemyer–Peppas shows the best fit ($R^2 = 0.9544$) compared to other kinetic model for the release of fragrance from nanocontainers.

Keywords Nanocontainers · Fragrance release · Halloysite · TEM · Kinetic models · pH

S. A. Ghodke · S. Mishra
University Department of Chemical Technology, North Maharashtra University, Jalgaon 425001, Maharashtra, India

S. H. Sonawane (✉)
Department of Chemical Engineering, National Institute of Technology, Warangal 506004, Andhra Pradesh, India
e-mail: shirishsonawane@rediffmail.com

B. A. Bhanvase
Department of Chemical Engineering, Laxminarayan Institute of Technology, Nagpur 440033, Maharashtra, India

K. S. Joshi
Department of Biotechnology, Sinhgad College of Engineering, Pune 411041, Maharashtra, India

Introduction

In recent times, targeted delivery of active molecules for various fields like corrosion inhibition, food processing, agriculture and drug delivery have gained more attention because of their sustainable release profiles [1, 2]. The active molecules for the targeted delivery may suffer from contamination, unwanted environment and rapid evaporation. Hence it becomes necessary to encapsulate the active molecules by a shell material that prevents their release and penetration of environmental factors until desired. This ensures the increased efficacy of delivery systems in this regard to its strength. To deliver these active molecules varieties of nano/micro containers have been synthesized by many researchers. These capsules prepared included use of materials such as protein [3], polyelectrolyte [4, 5], polymers [6] emulsions [7], suspension [8], corrosion inhibitor [9, 10].

Fragrance is a mixture of natural or synthetic essential oils or aroma compounds, additives and solvents. Fragrances are one of the essential components in food, leather, paper and textile as they produce sedative [11], tranquilization [12] and antibacterial [13] effects in the product. Many cosmetic products such as liquid cleansing compositions, skin care creams, antiperspirants are used effectively to deliver and/or deposit various benefit agents such as perfumes into and onto the skin. The primary

requirement of such products is fragrance longevity. The long lasting fragrance perception increases the product demand. The various natural and synthetic fragrant molecules are being synthesized or isolated from various applications. However, many of these fragrance molecules are unstable due to their reactive functionalities, such as aldehyde, ketone and terpenes. Encapsulation of fragrant molecules loaded on or in the hollow lumen of containers provides protection to the fragrant molecule to meet the desired objective of delivery. For the specific applications, fragrance delivery requires a carrier to hold the fragrant molecules and possess prolonged responsive controlled release. For this reason encapsulation of fragrant molecules was studied by many researchers using chitosan [14], bovine serum albumin [15] and polymers [8, 16].

The sizes of nanocontainer shell depend on the art of synthesis methodology. The time required for the shell synthesis varies from 4 to 24 h also the level of sophistication required which may affect the nanosphere size [14, 16, 17]. The selection of shell material is decided from the type of bulk medium in which active molecule is to be delivered. So it was essential to look for inexpensive, biocompatible nanocontainers with simple mean of fabrication. The inorganic nanomaterials such as zeolite and hydrotalcite were also studied for the delivery of enzymes but suffer from disadvantages such as small pore size and low surface area respectively [18, 19].

Halloysite is an economically viable clay material that can be mined from deposits as a raw mineral. Halloysite $[Al_2Si_2O_5(OH)_4X\ nH_2O]$ is a two-layered (1:1) aluminosilicate. Generally halloysite are mined from natural deposits and is similar to kaolin, but differs in having hollow microtubular rather than a stacked plate-like structure. The dimensions of halloysite tubules vary from 500 to 1,000 nm in length and 15–100 nm in inner diameter (lumen) depending on the deposit [20]. The first use of inexpensive and viable nanoscale halloysite as a container for the encapsulation was demonstrated in earlier studies [21] and a patent was also filed on the use of the material for the extended delivery of a range of biocides following incorporation into marine antifouling paints. Further the use of halloysite being a potential candidate for drug delivery was described and the physicochemical characterization of halloysite was carried out, to indicate its use in the production of novel drug delivery systems for drug and other agents [22]. The use of coated microtubular halloysite was studied for the sustained release of diltiazem hydrochloride used for the treatment of angina and hypertension and propranolol hydrochloride [23]. Coating with adequate polyethyleneimine was particularly effective at delaying drug release, being dependent on the architecture of the interaction between the polycation and the mineral.

Abdullayev et al. have discussed on halloysite tubes as nanocontainers for anticorrosion coating with benzotriazole [24]. Halloysite may be used as an additive in paints to produce a functional composite coating material. A maximum benzotriazole loading of 5 % by weight was achieved for clay tubes of 50 nm external diameters and lumen of 15 nm. Variable release rates of the corrosion inhibitor were possible in a range between 5 and 100 h, as was demonstrated by formation of stoppers at tube openings. The release of corrosion inhibitors encapsulated within nanocontainers, triggered by the corrosion process, was reported in earlier studies [25]. This technique prevented the spontaneous leakage of the corrosion inhibitor out of the coating. The study presented few methods for the fabrication of such nanocontainers, encapsulation of active materials and their permeability properties. Two more studies were published on use of halloysite in water treatment where in as adsorbent for cationic dye [26] and chromium VI [27]. The halloysite as enzyme biocatalyst was reported where two typical industrial enzymes (α-amylase and urease) with different sizes were immobilized in channels of the nanotubes through simple physical adsorption [28]. After 60 min heating, both immobilized enzymes retained more than 80 % activity. Stored for 15 days, the immobilized enzymes still show more than 90 % activity. More than 55 % initial activity of the enzyme was retained after seven cycles. In one of the corrosion protection studies [9], it was shown that polyacrylic acid formed a protective layer over a cargo deposited onto the nanocontainer and PAA layer produced a responsive release.

In the present study, we reported the use of halloysite nanocontainers for the prolonged release of fragrant molecules. The hollow lumen of halloysite was used as a cargo to deliver fragrant molecules and the nanocontainer was then coated with a polyelectrolyte to preserve the volatile fragrant molecule. These nanocontainers can be used in various personal care, cosmetic products and liquid cleansing compositions, for example perspiration causes fluid secretion which lies in the range of pH 4.5 to 7. Hence halloysite nanocontainers can be designed to fulfill the fragrance delivery with longevity. The objective of the study was to determine the overall prolonged fragrance delivery. Since the rose absolute used herein was completely miscible in water in all composition, the release concentration was determined using UV–Visible spectroscopy ($\lambda_{max} = 269$ nm). Effect of change in pH was also determined to study the release behavior. The nanocontainer was characterized by FTIR, Transmission Electron Microscopy (TEM) and TGA analysis. Various kinetic models related to release studies available in literature have been studied to determine kinetics of fragrance release from nanocontainers [29, 30]. A criterion for selecting the most

appropriate model was based on linearity (coefficient of correlation). Best fit for all the models were analysed for 0 to 60 min release and for 0 to 24 h release.

Materials and Methods

Materials

Halloysite tubes samples were obtained from Sigma Aldrich with outside diameter 30–50 nm, lumen 15 nm and length 800 ± 300 nm. Analytical grade chemical polyacrylic acid (PAA, $M_w = 50{,}000$ gmol^{-1}), was procured from Sigma Aldrich and used as received from the supplier. Demineralized water prepared using Millipore apparatus was used during all the experimental runs. Rose absolute was procured from local market without any purification. Phosphate buffer capsules were procured from MERC Specialties, Mumbai.

Characterization

FTIR spectra were recorded on Perkin Elmer FTIR Spectrometer (Paragon1000 PC) in the range 4,000–400 cm^{-1}. The morphology and structure of halloysite nanotubes was studied using TEM, which was performed on Technai G20 working at 200 kV. TGA was carried out using NETZSCHDSC 204, with a heating rate of 10 °C/min from room temperature to 700 °C and a dynamic nitrogen flow of 50 cm^3/min. The obtained samples were centrifuged in order to remove nanocontainer from the sample and then the sample was used for UV–Vis analysis. Solution concentration was determined by using UV–Vis spectrophotometer (SHIMADZU, UV-3600, India) at ambient temperature. The calibration plot was developed and the wavelength of maximum absorbance (λ_{max}) of solution was obtained as 269 nm using deionized water as reference. The pH of the solution was adjusted with HCl or NaOH solution by using a pH meter.

Loading Fragrance on Halloysite Nanocontainers

Before loading the nanocontainers with fragrance molecules the nanocontainers were dispersed in demineralized water and sonicated for 5 min. In the present study, ultrasound act as an intensified source of energy dissipation and shearing action generated by ultrasonic cavitation which helps in exfoliation and homogeneous dispersion of clay [31]. 20 g rose essence was dispersed in 1 L demineralized water to prepare the rosewater solution. 2 g Halloysite nanotubes were then added into 50 mL rosewater solution. The solution was evacuated by means of vacuum pump for 30 min (vacuum 27″ Hg, pressure 35 psi, motor 1/16 HP). The evacuation was repeated thrice to ensure adequate loadings of fragrance molecules in the nanotubes. The mixture was then centrifuged at 1,000 rpm for 20 min. The supernatant was removed and the fragrance loaded Halloysite nanotubes were obtained.

Deposition of Polyelectrolyte Layer

In order to restrict the volatilization of fragrance molecule, it was necessary to cover the shell material. For this reason, a thin coat of polyelectrolyte (PAA) was achieved on fragrance loaded nanocontainers using 2 mg mL^{-1} PAA solution for a period of 20 min. Finally the nanocontainers were separated by centrifugation followed by drying at 45 °C for 24 h. This layer of polyelectrolyte served as a protective barrier against release of fragrance molecules. The fragrance loaded into the hollow lumen and prolongs release of fragrance molecules was achieved using a protective polyelectrolyte layer, as schematically outlined in Fig. 1.

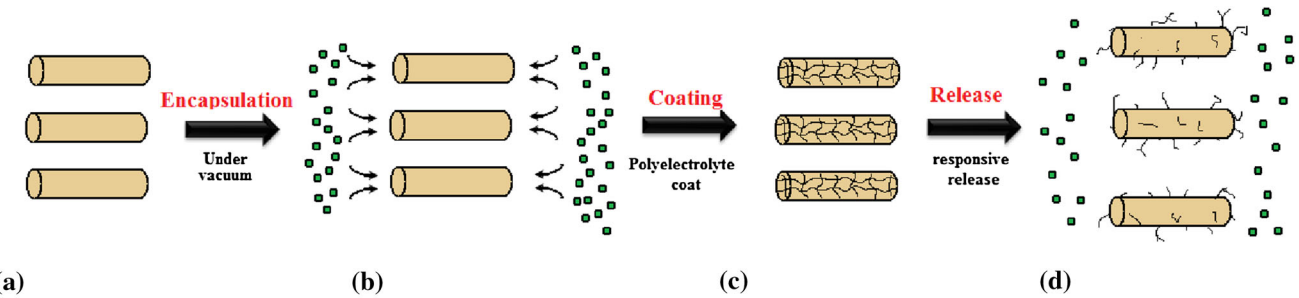

Fig. 1 Schematic illustration of the procedure for loading and release of fragrance in halloysite nanocontainers (**a**) halloysite nanocontainers, (**b**) encapsulation procedure under vacuum where fragrance molecules enter in the lumen (**c**) coating thin layer of polyelectrolyte on the surface of nanocontainers (**d**) responsive release of fragrance molecules in acidic environment

Fragrance Release Studies

The fragrance release studies were performed in a batch reactor at room temperature. During batch experiments, 1 g PAA coated fragranced nanocontainers were added to a 100 mL de-ionized water of desired pH. The mixture was stirred at a constant speed and pH of reaction mixture was adjusted using a phosphate buffer. The release of fragrance molecules was monitored for 24 h and release data was obtained. The samples were collected at definite interval and were analyzed for using UV–Visible spectrophotometer. The release studies were monitored for overall fragrance release and not for a specific compound. Reproducibility of the results was checked by repeating the experiments and was found satisfactory with the experimental error within ±5 %.

Kinetic Models for Release Study

The release profiles were fitted to Zero order model (Eq. 1), First order model (Eq. 2), Higuchi model (Eq. 3), Hixson-Crowell model (Eq. 4), Hopfenberg model (Eq. 5) and Korsemeyer-Peppas model (Eq. 6).

$$Q_t - Q_0 = K_0 t, \tag{1}$$

where Q_0 is the initial amount of active molecule in the delivery system form, Q_t is the amount of fragrance in nanocontainer dosage form at time t and K_0 is a proportionality constant [32]

$$\ln \frac{M_t}{M_\infty} = -Kt, \tag{2}$$

where M_t is the concentration of fragrance present in nanocontainer at time t, M_∞ is the initial concentration of fragrance in nanocontainer, K is the first order rate constant (time^{-1}) [33]

$$Q_t = K_H t^{1/2}, \tag{3}$$

where Q_t is the amount of fragrance released in time t, K_H is the Higuchi dissolution constant [34]

$$W_0^{1/3} - W_t^{1/3} = K_s t, \tag{4}$$

where W_t is the remaining amount of fragrance in nanocontainer at time t, W_0 is the initial amount of fragrance in nanocontainer, K_s is the constant incorporating the surface-volume relation [35]

$$1 - (1 - Q_t/Q_\infty)^{1/n} = k_1 t \tag{5}$$

Q_t = amount of fragrance released in time t, Q_∞ = amount of fragrance released in the solution at infinite time, k_1 = erosion rate constant [35].

Fickian diffusion release from a thin polymer film is given by [36],

$$\frac{\partial C}{\partial t} = D\frac{\partial^2 C}{\partial x^2} \tag{6}$$

where,

$t = 0$	$-l/2 < x < l/2$	$C = C_1$
$t > 0$	$x = \pm l/2$	$C = C_0$

C_1 is initial uniform drug concentration of solution and C_0 is the concentration of solute at the surface of the slab.

Semi-empirical equation for drug release from thin polymer slabs is given by [37],

$$Q_t/Q_0 = k_t t^n \tag{7}$$

Q_t = amount of fragrance released in time t, Q_0 = initial amount of fragrance in the solution, k_t = release rate constant, n = release exponent which is indicative of transport mechanism [36]. Fickian diffusion is defined by n = 0.50 and non-Fickian by n > 0.50.

To find the Regression coefficients (R^2) data was plotted as follows:

Zero order kinetic model:	Q_t vs. t
First order kinetic model:	$\ln(M_t/M_\infty)$ vs. t
Higuchi model:	Q_t vs. $t^{1/2}$
Hixson-Crowell:	$W_0^{1/3} - W_t^{1/3}$ vs. t
Hopfenberg model:	$1 - (1 - Q_t/Q_\infty)^{1/n}$ vs. t
Korsemeyer-Peppas model:	$\ln(Q_t/Q_0)$ vs.$\ln(t)$

Results and Discussion

FTIR Analysis of Nanocontainers

Halloysite nanotubes were used as template for halloysite containers which act as a delivery vehicle for the fragrance molecules in order to obtain a prolong release of fragrance molecules. The FTIR spectrum of halloysite nanotubes, fragrance loaded halloysite nanocontainres and PAA coated fragranced nanocontainers are shown in Fig. 2. In this pattern peaks at 1008, 1030, 1114 cm^{-1} correspond to Si–O stretching region. The presence of characteristics peaks at 3,620 and 3,695 cm^{-1} indicated the presence of O–H group of inner surface of halloysite nanotubes. Stretching mode of Si–O bond is attributed to the characteristics peak at 1,111 cm^{-1}. The peak was observed at 540 cm^{-1} which indicated the presence of Al–O–Si bond. The inner surface hydroxyl groups were also indicated by a peak at 920 cm^{-1} [38]. Figure 2 (pattern B) showed FTIR spectrum of fragrance loaded halloysite nanocontainer. No major change in prominent peaks of nanocontainers, were observed, which implied that encapsulated fragrance molecules were not present on the surface of the nanocontainers. The surface of

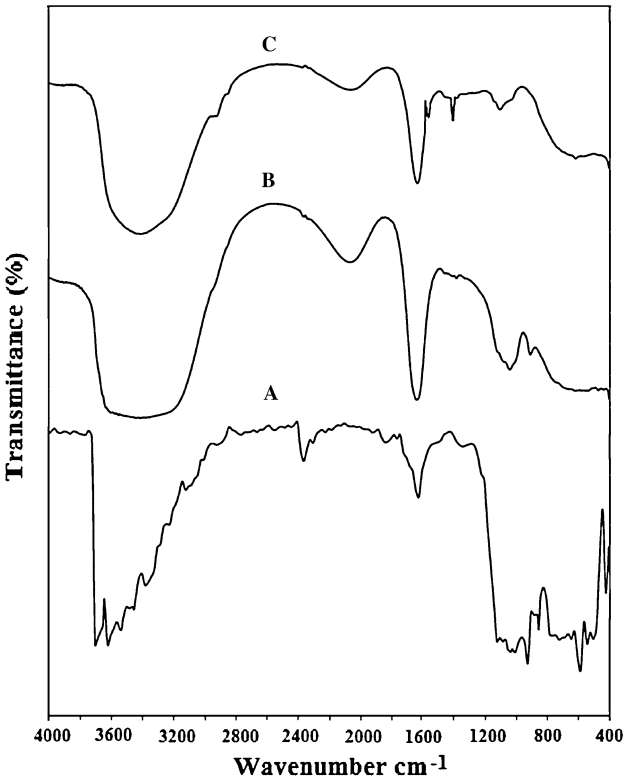

Fig. 2 FTIR spectra of (**A**) Halloysite nanocontainers (**B**)Fragrance loaded nanocontainers (**C**) PAA coated fragranced nanocontainers

nanocontainers was then coated with a thin layer of PAA. Figure 2 (pattern C) depicted FTIR spectrum for Polyelectrolyte (PAA) coated fragranced nanocontainers. The peak was obtained at 1,560 cm^{-1}, which indicated C=O stretching and the peak at 1,410 cm^{-1} corresponding to C–O–H in-plane bending indicated the presence of PAA [39]. Another broad peak is observed at 2,600 cm^{-1} indicating the existence of O–H stretching.

TEM Analysis of Nanocontainer

TEM was used to determine the shape and the size of halloysite nanocontainers. TEM image of halloysite nanocontainer with a hollow tubular morphology with 30–50 nm diameter and 800–1,000 nm length tubules is shown in Fig. 3. The hollow tubule area was used to house the fragrance molecules on which thin coating layer of PAA was accomplished in order to hold fragrance molecules in halloysite nanocontainer. The halloysite tubes, filled with fragrance molecules, was observed in TEM image.

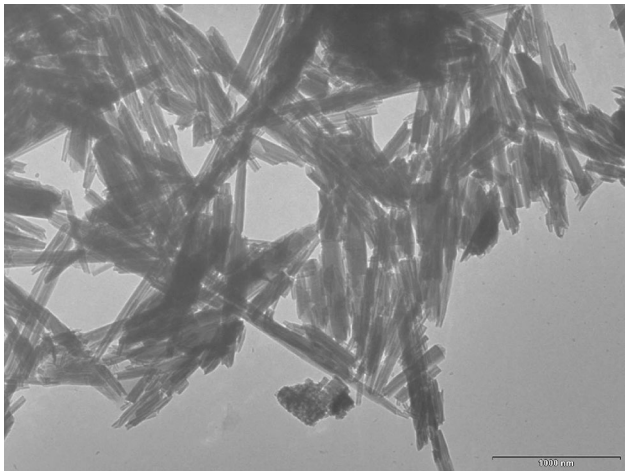

Fig. 3 TEM image of halloysite nanocontainers

UV–Visible Spectra

The optical properties are strongly dependent on the particle size. Absorption spectra of fragrance, halloysite nanotubes, fragrance loaded halloysite nanocontainers and polyelectrolyte coated fragranced halloysite nanocontainers are depicted in Fig. 4. Pattern A of Fig. 4 shows absorption spectra for aqueous solution of fragrance. Pattern B and C of Fig. 4 depict absorption spectra for halloysite nanotubes and fragrance loaded halloysite nanocontainers indicating no size change during encapsulation process. Pattern D of Fig. 4 shows an increase in the size of halloysite nanocontainer with loading of thin layer of PAA on fragrance loaded halloysite nanocontainer. This layer

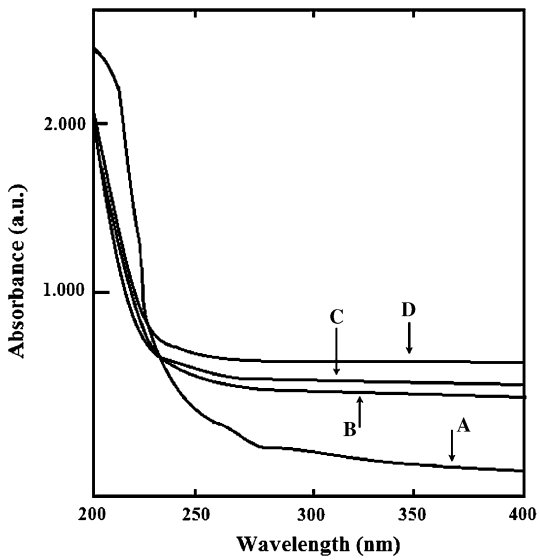

Fig. 4 Absorption spectra of (**A**) Pure fragrance, (**B**) Halloysite nanotubes, (**C**) Fragrance loaded halloysite nanocontainer and (**D**) PAA coated fragranced nanocontainers

worked as a protective barrier of PAA on the outer surface of nanocontainers.

TGA Analysis of Nanocontainers

The thermal stability of halloysite nanotubes and PAA coated fragranced nanocontainers was evaluated using TGA. Figure 5 (pattern A) shows that the first stage weight loss (around 4 %) at lower temperature (30 to 140 °C) due to physically adsorbed water attributed to O–H bond. This has been also reported in FTIR analysis section. The weight loss at higher temperature (more than 140 °C) was result of the dehydration and dehydroxylation of the clay sheet [40], which implied a good thermal stability of inorganic material at higher temperatures. Figure 5 (pattern B) shows the TGA curve for coated fragranced halloysite nanocontainers. The first stage (30 to 140 °C) weight loss (about 6 %) was attributed to the evaporation of physically absorbed water and release of moieties based on aromatic ions. The second weight loss stage started at 150 °C which was attributed to anhydride formation and decarboxylation and the degradation continues further. The reduction in the weight was an indication of successful loading of significant amount of fragrance molecules in the halloysite nanocontainers.

Release Study of Fragrance from PAA Coated Fragranced Halloysite Nanocontainers

As the fragrance molecules tend to release very quickly due to its volatile nature, the fragrances lifetime was increased with the help of thin coat of a polyelectrolyte like PAA. Also for variety of delivery system applications, it becomes necessary to achieve its responsive release. The present nanocontainers can be used in fragrance delivery products like deodorants, sprays and so on. These products are aimed to remove unwanted smell produced due to perspiration which is acidic. Therefore release performance of fragrance was evaluated in aqueous acidic medium. Figure 6 indicates the release of fragrance from fragrance loaded halloysite nanocontainer at various pH values at room temperature and depicts that the prepared nanocontainers shows proper encapsulation of fragrance into nanocontainers. The release study was carried out for 24 h but there was no significant release after 5 h and reaches steady state, therefore release rates of 5 h studies are only reported. The release concentration of fragrance was found to be increased with decrease in the aqueous medium pH. This showed the release rate of fragrance molecules was more in acidic medium (lower pH values). It was also found that the release of fragrance molecules increased with respect to time, then it was found to be constant at equilibrium [9, 10]. It was due to decrease in diffusion rate of fragrance with decrease in the concentration gradient, with respect to exposure time. Also at lower pH, the inner lumen with positive charge, was found to produce more and more repulsion between moieties resulting into more fragrance release. Further Fig. 6 shows an increasing trend of fragrance release at all pH values with respect to time. Maximum release at 5 h (150 mg of fragrance release mg l^{-1} g^{-1} of nanocontainers) was found in case of operating pH of 3, while only a minimal release (103 mg of fragrance release mg l^{-1} g^{-1} of nanocontainers) was observed at pH 7 at the end of 5 h.

Kinetic Model Analysis for Fragrance Release from Halloysite Nanocontainer

The data for release of fragrance from halloysite nanocontainer at various pH with respect to time was fitted to Zero Order Model (Eq. 1), First Order Model (Eq. 2), Higuchi Model (Eq. 3), Hixson-Crowell Model (Eq. 4), Hopfenberg Model (Eq. 5) and Korsemeyer Peppas Model (Eq. 7). Figure 7 depicted the application of Zero order

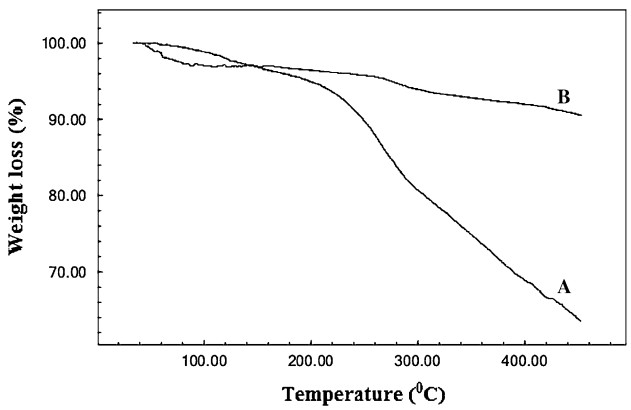

Fig. 5 TGA curves of halloysite nanocontainers (**A**) and Polyelectrolyte (PAA) coated fragranced nanocontainers (**B**)

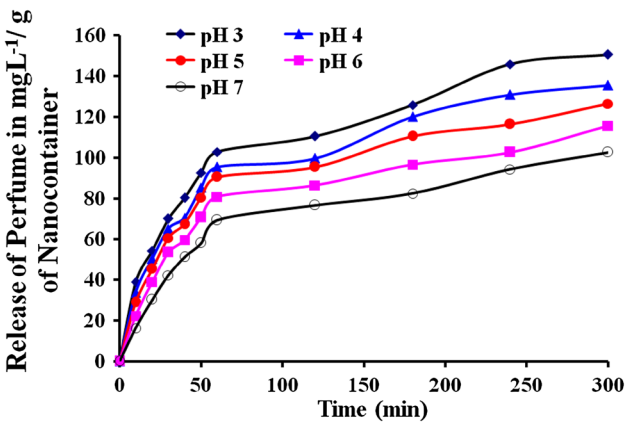

Fig. 6 Release of fragrance from 1 g Polyelectrolyte (PAA) coated fragranced nanocontainers at different pH at room temperature

model for fitting the fragrance release data from halloysite nanocontainer. The zero order fragrance release constant was established to be in the range of 0.656–0.435 mg/l min for the pH change from 3 to 7. Similarly Figs. 8, 9, 10, 11 and 12 show the fragrance release data fitting to First order, Higuchi, Hixon-Crowell, Hopfenberg and Korsmeyer-Peppas release models. The respective rate constants and R^2 values are reported in Table 1. In all the cases the constant parameter was found to be decreased with increase in the pH value form 3 to 7 indicating that more release in acidic region for better fragrance release properties. Figures 7, 8, 9, 10, 11, 12 and Table 1 indicate that the Korsmeyer–Peppas Kinetic Release Model to be the best fit, compared to other empirical models.

Equation (6) gives Fickian diffusion release from a thin polymer film. This model described typical experimental conditions for release experiments and assumed one dimensional isothermal solute release from a thin polymer slab of thickness *l*. For short time behavioural analysis, the equation can be solved into trigonometric series under boundary conditions. It was found that the short time approximation was valid only for first 60 % of total released species [36]. Semi-empirical equation for species, released from thin polymer slabs was used to express the general species behaviour (Eq. 7). Fickian and non-Fickian diffusion were defined by $n = 0.50$ and $n > 0.50$ respectively. Korsmeyer et al. have developed a simple, semi-empirical model (Eq. 7), for the drug release to the elapsed time (t) [37, 41]. In this model, the value of n characterizes the release mechanism of drug. For cylindrical tablets, $0.45 \leq n$, $n < 0.89$, $n = 0.89$ and $n > 0.89$ corresponding to Fickian diffusion mechanism, non-Fickian transport, Case II (relaxational) transport and Super case II transport respectively. Korsemeyer–Peppas release model of fragrance release from polyelectrolyte coated fragranced nanocontainers during 0 to 300 min is shown in Fig. 12. The graph shows the coefficient values tend to decrease with increase in pH from 3 to 7 and all the values are found to be nearer to $n = 0.4$ indicating Fickian diffusion mechanism.

From the plausible mechanism (Fig. 1), the water dissolved the polyelectrolyte layer and further permeated into the nanocontainer for releasing the fragrance molecules into the surrounding. This produced nanocontainers, immediately occupied by water, which allows diffusion of fragrance molecules into the surrounding. Therefore, the presence of polyelectrolyte layer can produce slower release as compared to coated nanocontainer. The release results were analysed with the various model fitting,

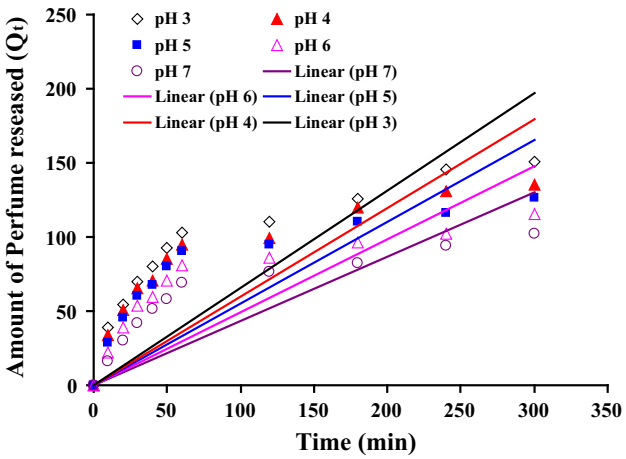

Fig. 7 Zero Order Release Model for fragrance release from polyelectrolyte coated fragranced nanocontainers at different pH

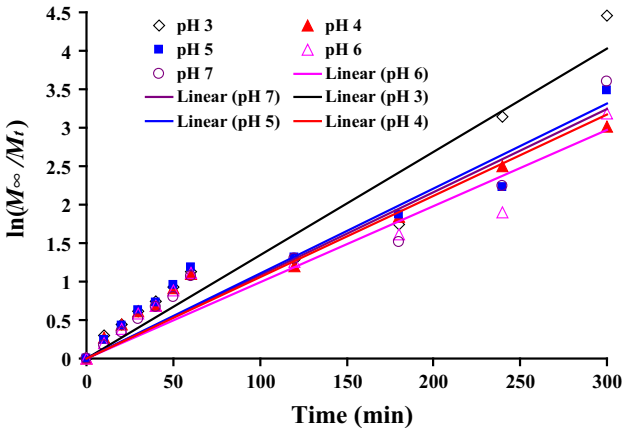

Fig. 8 First Order Release Model for fragrance release from polyelectrolyte coated fragranced nanocontainers at different pH

Table 1 Release kinetic data for polyelectrolyte coated fragranced nanocontainers at different pH values

pH	Zero order		First order		Higuchi model		Hixson–Crowell		Hopfenberg		Korsemeyer–Peppas		
	K_0	R^2	K	R^2	K_H	R^2	K_S	R^2	K_1	R^2	K_t	R^2	n
3	0.6560	0.0964	0.0134	0.9412	9.9630	0.8845	0.0147	0.8569	0.0034	0.7284	0.1209	0.9544	0.3813
4	0.5970	0.0758	0.0106	0.9290	9.0850	0.8762	0.0128	0.7645	0.0031	0.6322	0.1154	0.9445	0.3863
5	0.5515	0.0437	0.0111	0.9141	8.4110	0.8598	0.0127	0.7565	0.0032	0.6169	0.1105	0.9211	0.3984
6	0.4930	0.1182	0.0099	0.8865	7.4840	0.8733	0.0115	0.7438	0.0030	0.6200	0.0923	0.9018	0.4281
7	0.4350	0.3062	0.0108	0.9279	6.5350	0.9173	0.0115	0.8456	0.0031	0.7473	0.0697	0.9060	0.4851

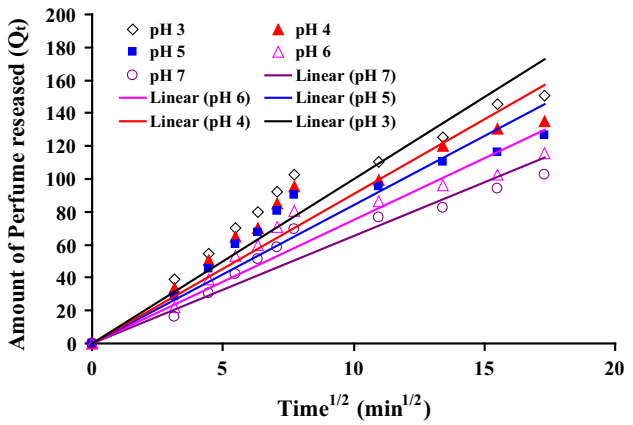

Fig. 9 Higuchi Release Model for fragrance release from polyelectrolyte coated fragranced nanocontainers at different pH

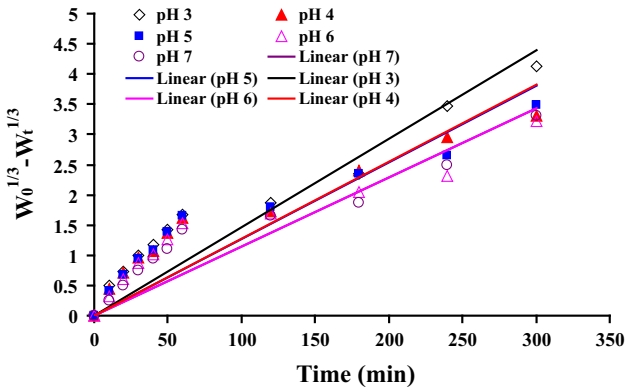

Fig. 10 Hixson-Crowell Release Model for fragrance release from polyelectrolyte coated fragranced nanocontainers at different pH

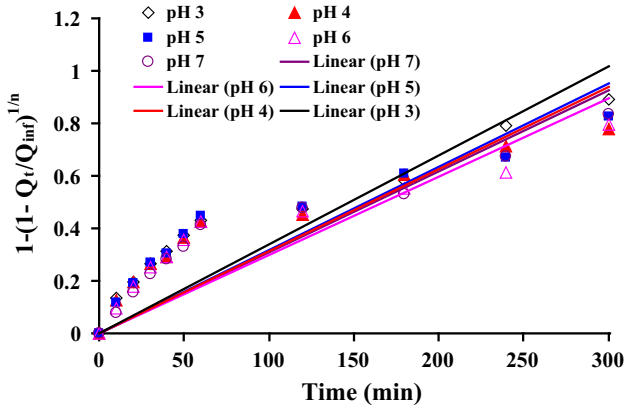

Fig. 11 Hopfenberg Release Model for fragrance release from polyelectrolyte coated fragranced nanocontainers at different pH

wherein goodness of the fit was determined. Korsemeyer–Peppas model studied herein described the fragrance release and the geometry of the nanocontainer. The model results indicated that the fragrance release was dependent

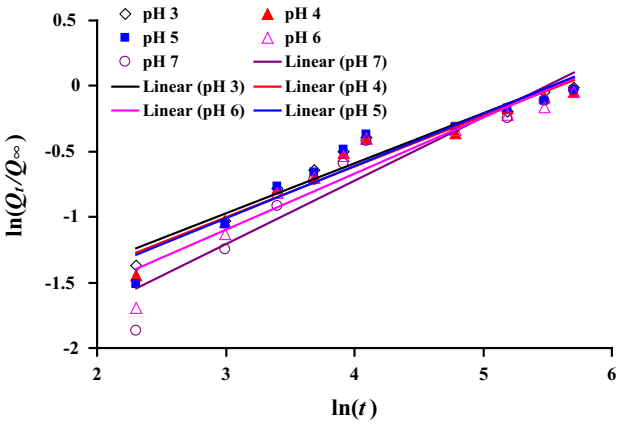

Fig. 12 Korsemeyer–Peppas Release Model for fragrance release from polyelectrolyte coated fragranced nanocontainers at different pH

on time and initial concentration of nanocontainers in the given system.

Conclusions

The loading of fragrance molecules in polyelctrolyte coated fragranced nanocontainers were successfully accomplished using the reported method. The results of FTIR, TEM, TGA and UV spectrum confirmed the formation of coated cylindrical Halloysite nanocontainers. The diameter and length of nanocontainers was found to be 30–50 nm and 500–800 nm respectively. The coated fragranced nanocontainers were subjected for a 24 h release studies and it was found to be consistent after 5 h time. The fragrance release was found to be responsive, the amount of fragrance release increased with decrease in pH. Therefore the release of fragrance was quantitatively analyzed successfully from Halloysite nanocontainers using six different kinetic models like zero order, first order, Hixson–Crowell, Higuchi, Korsmeyer–Peppas and Hopfenberg release models available in the literature. It is established that the Korsmeyer–Peppas release model is best among the six models used to predict the fragrance release from Halloysite nanocontainers. It is also found that the parameter estimated i.e. '*n*' for Korsemeyer Peppas model is around 0.4 indicating Fickian diffusion mechanism. Finally the coated fragranced nanocontainers are found to be responsive and promising for the fragrance delivery applications in personal care and cosmetic products.

References

1. M.L. Zheludkevich, J. Tedim, M.G.S. Ferreira, "Smart" coatings for active corrosion protection based on multi-functional micro and nanocontainers. Electrochim. Acta **82**, 314–323 (2012)

2. E. Fleige, M.A. Quadir, R. Haag, Stimuli-responsive polymeric nanocarriers for the controlled transport of active compounds: concepts and applications. Adv. Drug Deliver. Rev. **64**, 866–884 (2012)
3. M. Zhou, T.S.H. Leong, S. Melino, F. Cavalieri, S. Kentish, M. Ashokkumar, Sonochemical synthesis of liquid-encapsulated lysozyme microspheres. Ultrason. Sonochem. **17**, 333–337 (2010)
4. D.G. Shchukin, K. Kohler, H. Mohwald, G.B. Sukhorukov, Gas-filled polyelectrolyte capsules. Angew. Chem. Int. Edit. **44**, 3310–3314 (2005)
5. D.G. Shchukin, D.A. Gorin, H. Mohwald, Ultrasonically induced opening of polyelectrolyte microcontainers. Langmuir **22**, 7400–7404 (2006)
6. D. Horák, M. Trchová, M.J. Bene, M. Veverk, E. Pollert, Monodisperse magnetic compo site poly(glycidyl methacrylate)/$La_{0.75}Sr_{0.25}MnO_3$ microspheres by the dispersion polymerization. Polymer **51**, 3116–3122 (2010)
7. F. Tiarks, K. Landfester, M. Antonietti, Preparation of polymeric nanocapsules by miniemulsion polymerization. Langmuir **17**, 908–918 (2010)
8. L. Sanchez, P. Sanchez, A. De-Lucas, M. Carmona, J.F. Rodriguez, Microencapsulation of phase change materials with a polystyrene shell. Colloid Polym. Sci. **285**, 1377–1385 (2007)
9. S.H. Sonawane, B.A. Bhanvase, A.A. Jamali, S.K. Dubey, S.S. Kale, D.V. Pinjari, A.B. Pandit, Improved active anticorrosion coatings using layer-by-layer assembled ZnO nanocontainers with benzotriazole. Chem. Eng. J. **189–190**, 464–472 (2012)
10. B.A. Bhanvase, Y. Kutbuddin, R.N. Borse, N. Selokar, D.V. Pinjari, S.H. Sonawane, A.B. Pandit, Ultrasound assisted intensification of calcium zinc phosphate pigment synthesis and its nanocontainer for active anticorrosion coatings. Chem. Eng. J. **231**, 345–354 (2013)
11. S.Q. Li, J.E. Lewis, N.M. Stewart, L. Qian, H.J. Boyter, Effect of finishing methods on washing durability of microencapsulated aroma finishing. J. Textile Inst. **99**, 177–183 (2008)
12. N. Gordon, Microencapsulation in textile finishing. Rev. Prog. Color. Rel. Top. **321**, 57–64 (2001)
13. G. Kyle, Evaluating the effectiveness of aromatherapy in reducing levels of anxiety in palliative care patients: results of a pilot study. Complement. Ther. Clin. Pract. **12**, 148–155 (2006)
14. T. Tree-udom, S.P. Wanichwecharungruang, J. Seemork, S. Arayachukeat, Controlled release systems with physical and chemical barriers. Carbohyd. Polymers. **86**, 1602–1609 (2011)
15. O. Tzhayik, A. Cavaco-Paulo, A. Gedanken, Fragrance release profile from sonochemically prepared protein microsphere containers. Ultrason. Sonochem. **19**, 858–863 (2012)
16. B. Peña, C. Panisello, G. Aresté, R. Garcia-Valls, T. Gumí, Preparation and characterization of polysulfone microcapsules for fragrance release. Chem. Eng. J. **179**, 394–403 (2012)
17. P. Wang, D. Wang, T. Xie, H. Li, M. Yang, X. Wei, Preparation of monodisperse Ag/Anatase TiO_2 core–shell nanoparticles. Mater. Chem. Phy. **109**, 181–183 (2008)
18. S. Martinez-Gallegos, S. Bulbulian, Effects of γ radiation on chromate immobilization by calcined hydrotalcites. Clay. Clay. Min. **52**, 650–656 (2004)
19. A. Corma, V. Fornes, F. Rey, Delaminated zeolites: an efficient support for enzymes. Adv. Mat. **14**, 71–74 (2002)
20. Y.M. Lvov, D.G. Shchukin, H. Mohwald, R.R. Price, Halloysite clay nanotubes for controlled release of protective agents. ACS Nano **2**, 814–820 (2008)
21. R.R. Price, B.P. Gaber, Y.M. Lvov, In-vitro release characteristics of tetracycline HCl, khellin and nicoti-namide adenine dineculeotide from halloysite. A cyclindrical mineral. J. Microencap. **18**, 713–722 (2001)
22. S.R. Levis, P.B. Deasy, Characterisation of halloysite for use as a microtubular drug delivery system. Int. J. Pharma. **243**, 125–134 (2002)
23. S.R. Levis, P.B. Deasy, Use of coated microtubular halloysite for the sustained release of diltiazem hydrochloride and propranolol hydrochloride. Int. J. Pharm. **145**, 145–157 (2003)
24. E. Abdullayev, R. Price, D. Shchukin, Y. Lvov, Halloysite tubes as nanocontainers for anticorrosion coating with benzotriazole. Appl. Mater. Interf. **1**, 1437–1443 (2009)
25. D.V. Andreeva, D.G. Shchukin, Smart self-repairing protective coatings. Mater. Today **11**, 24–30 (2008)
26. R. Liu, B. Zhan, D. Mei, H. Zhang, J. Liu, Adsorption of methyl violet from aqueous solution by halloysite nanotubes. Desalination **268**, 111–116 (2011)
27. W. Jinhua, Z. Xiang, Z. Bing, Z. Yafei, Z. Rui, L. Jindun, C. Rongfeng, Rapid adsorption of Cr(VI) on modified halloysite nanotubes. Desalination **259**, 22–28 (2010)
28. R. Zhai, B. Zhang, L. Liu, Y. Xie, H. Zhang, J. Liu, Immobilization of enzyme biocatalyst on natural halloysite nanotubes. Catal. Commun. **12**, 259–263 (2010)
29. A.B. Lokhande, S. Mishra, R.D. Kulkarni, J.B. Naik, Influence of different viscosity grade ethylcellulose polymerson encapsulation and in vitro release study of drug loaded nanoparticles. J. Pharmacy Res. **7**, 414–420 (2013)
30. J. Suksaeree, P. Boonme, W. Taweepred, G. Ritthidej, W. Pichayakorn, Characterization, in vitro release and permeation studies of nicotine transdermal patches prepared from deproteinized natural rubber latex blends. Chem. Eng. Res. Des. **90**, 906–914 (2012)
31. B.A. Bhanvase, D.V. Pinjari, P.R. Gogate, S.H. Sonawane, A.B. Pandit, Synthesis of exfoliated poly(styrene-co-methyl methacrylate)/montmorillonite nanocomposite using ultrasound assisted in situ emulsion copolymerization. Chem. Eng. J. **181–182**, 770–778 (2012)
32. C.G. Varelas, D.G. Dixon, C. Steiner, Zero-order release from biphasic polymer hydrogels. J. Control. Release **34**, 185–192 (1995)
33. A. Silvina, M. Bravo, C. Lamas, J. Claudio, In vitro studies of diclofenac sodium controlled —release from biopolymeric hydrophillic matrices. J. Pharm. Pharm. Sci. **5**, 213–219 (2002)
34. M.A. Hadi, A.S. Rao, S. Martha, Y. Sirisha, P.U. Chandrika, Development of a floating multiple unit controlled release beads of zidovudine for the treatment of AIDS. J. Pharm. Res. **6**, 78–83 (2013)
35. P. Costa, J.M. Lobo, Modeling and comparison of dissolution profiles. European J. Pharm. Sci. **13**, 123–133 (2001)
36. P.L. Ritger, N.A. Peppas, A simple equation for description of solute release I. Fickian and non-fickian release from non-swellable devices in the form of slabs, spheres, cylinders or discs. J. Control. Release **5**, 23–36 (1987)
37. V.N. Ravella, R.R. Nadendla, N.C. Kesari, Design and evaluation of sustained release pellets of aceclofenac. J. Pharm. Res. **6**, 525–531 (2013)
38. S. Bordeepong, D. Bhongsuwan, T. Pungrassami, T. Bhongsuwan, Characterization of halloysite from Thung Yai District, Nakhon Si Thammarat Province, in Southern Thailand, Songklanakarin. J. Sci. Tech. **33**, 599–607 (2011)
39. S.H. Sonawane, P.L. Chaudhari, S.A. Ghodke, M.G. Parande, V.M. Bhandari, S. Mishra, R.D. Kulkarni, Ultrasound assisted synthesis of polyacrylic acid–nanoclay nanocomposite and its application in sonosorption studies of malachite green dye. Ultrason. Sonochem. **16**, 351–355 (2009)
40. A.K. Panda, B.G. Mishra, D.K. Mishra, R.K. Singh, Effect of sulphuric acid treatment on the physico-chemical characteristics of kaolin clay. Colloids Surf. A **98**, 98–104 (2010)
41. R.W. Korsmeyer, R. Gurny, E.M. Doelker, P. Buri, N.M. Peppas, Mechanism of solute release from porous hydrophilic polymers. Int. J. Pharm. **15**, 25–35 (1983)